Propagation of Biochirality: Crossovers and Nonclassical Crystallization Kinetics of Aspartic Acid in Water

TU LEE,* YU KUN LIN, YA CHUNG TSAI, AND HUNG LIN LEE
Department of Chemical and Materials Engineering, National Central University, Jhong-Li City, Taiwan, R.O.C.

ABSTRACT All experimental procedures discussed could be treated as a screening tool for probing the existence of molecular association among the chiral molecules and the solvent system. The molecular association phases of a racemic conglomerate solution (CS) and a racemic compound solution (RCS), and the templating effect of aspartic acid solid surface were observed to minimize the chance of redissolving racemic conglomerate and racemic compound aspartic acid in water and reforming an RCS in crossovers experiments. Only 1 %wt% of *l*-aspartic acid was adequate enough to induce a transformation from a racemic compound aspartic acid to a racemic conglomerate aspartic acid. This would make the propagation of biochirality more feasible and sound. However, tetrapeptide, (*l*-aspartic acid)$_4$, failed to induce enantioseparation as templates purely by crystallization. Nonclassical crystallization theory was needed to take into account the existence of a CS. Fundamental parameters of the crystallization kinetics such as the induction time, interfacial energy, Gibbs energetic barrier, nucleation rate, and critical size of stable nuclei of: (i) racemic compound aspartic acid, (ii) racemic compound aspartic acid seeded with 1 %wt% *l*-aspartic acid, (iii) racemic conglomerate aspartic acid, and (iv) *l*-aspartic acid were evaluated and compared with different initial supersaturation ratios. Morphological studies of crystals grown from the crystallization kinetics were also carried out. *Chirality 25:768–779, 2013.*

KEY WORDS: racemic conglomerate solution; racemic compound solution; tetrapeptide; aspartic acid; crossovers; enantioseparation; templating effect

INTRODUCTION

Statistical analyses demonstrated only about 5 to 10% of the racemates form conglomerates,[1] and aspartic acid falls into the remaining 90% category of a racemic forming system as evidenced by (i) the seeding experiment,[2] and (ii) the solubility test.[2] Several interesting cases such as (*R*,*S*)-2-chloromandelic acid, free base of venlafaxine, and disulfide-based iodoplumbate, whose solid state transition depending on the crystallization conditions can take place either from a racemic compound to a racemic conglomerate or vice versa.[3–5]

Intriguingly, when aspartic acid was crystallized from solutions inside porous media, racemic conglomerate crystals of *d*- and *l*-aspartic acid were always produced.[6] Recently, we have also discovered the unusual molecular association of aspartic acid enantiomers in water forming a "racemic conglomerate solution" (CS). CS might have offered an opportunity for converting the thermodynamically stable racemic compound aspartic acid[7] into the metastable racemic conglomerate in water by either rapid acid–base reactions or antisolvent crystallization with cooling, without being concerned about its back conversion later to a racemic compound for quite some time![2] As a result, symmetry breaking and chiral enrichment of aspartic acid by preferential crystallization should have been very common and easy to occur near the sandy seashores and the hot volcanic areas on the primitive earth[2] when the process was further coupled with homochirogenesis of aspartic acid at 90°C[8] and chiral transmission.[9]

However, the birth of the first generation of left-handed aspartic acid have invoked a few questions with regard to the propagation of biochirality—the birth of the second and other generations of left-handed aspartic acid. For example, could racemic conglomerate and racemic compound aspartic acid be redissolved in water and reformed into a racemic compound solution even if the two forms have previously been separated by chance?[10] How could a regional enantioseparation of aspartic acid have propagated to a global event? Was crystallization or polymerization of aspartic acid responsible for propagation of biochirality?[11,12]

Therefore, the aim of this article is to address those questions by looking at the consequences of the crossovers among racemic conglomerate aspartic acid, enantiomeric aspartic acid (i.e., *l*-aspartic acid), tetrapeptide (i.e., (*l*-asp)$_4$), and racemic compound aspartic acid in water. The crystallization kinetics of: (i) racemic compound aspartic acid, (ii) racemic compound aspartic acid seeded with 1 %wt% of *l*-aspartic acid, (iii) racemic conglomerate aspartic acid, (iv) *l*-aspartic acid compound, and (v) racemic compound aspartic acid seeded with 1 %wt% of (*l*-asp)$_4$, were monitored and determined by electrical conductance. To avoid the temperature effect on conductivity measurements, antisolvent acetone was added into all water-based systems.

Additional Supporting Information may be found in the online version of this article.

Contract grant sponsor: National Science Council of Taiwan, R. O. C; Contract grant number: NSC-98-2113-M-008-006.

*Correspondence to: Tu Lee, Department of Chemical and Materials Engineering, National Central University, 300 Jhong-Da Road, Jhong-Li City 320, Taiwan, R.O.C. E-mail: tulee@cc.ncu.edu.tw

Received for publication 7 August 2012; Accepted 23 May 2013
DOI: 10.1002/chir.22212
Published online 19 July 2013 in Wiley Online Library (wileyonlinelibrary.com).

MATERIALS AND METHODS

Chemicals

d-(−)-aspartic acid ($C_4H_7NO_4$, purity 99%, mp = 300°C, MW = 133.1, ee (GLC): 98%, lot 03610DJ), *dl*-(±)-aspartic acid ($C_4H_7NO_4$, purity 99%, mp = 280°C, MW = 133.1, lot 029K0053), *l*-(+)-aspartic acid ($C_4H_7NO_4$, purity 98%, mp = 300°C, MW = 133.1, ee (GLC): 98%, lot 066K0184), $(l\text{-asp})_4$ ($C_{16}H_{22}N_4O_{13}$, purity of 97% , MW = 478.4, lot 089K1083), *d*-(−)-alanine ($C_3H_7NO_2$, purity 98%, mp = 291°C, MW = 89.09, lot 107 K1536), *dl*-(±)-alanine ($C_3H_7NO_2$, purity 99%, mp = 295°C, MW = 89.09, lot 108K0115), *l*-(+)-alanine ($C_3H_7NO_2$, purity 98%, mp = 314.5°C, MW = 89.09, lot 0001440397) and succinic acid ($C_4H_6O_6$, purity 99%, mp = 185° to 188°C, MW = 118.09, lot 058K0706) were all obtained from Sigma-Aldrich (St. Louis, MO).

Solvents

Acetone (CH_3COCH_3, purity 99.5%, bp = 56°C, MW = 58.09, lot AA-1101) was purchased from Cecho (Miaoli, Taiwan). Reversible osmosis (RO) water was clarified by a water purification system (model Milli-RO Plus) bought from Millipore (Billerica, MA).

Instrumentations

Fourier transform infrared spectroscopy (FTIR). Transmission Fourier transform infrared (FTIR) spectroscopy[13–15] was used to distinguish between a racemic conglomerate and a racemic compound of all dried solids based on IR assignments. IR spectra were recorded on a Perkin Elmer Spectrum One spectrometer (Perkin Elmer Instruments, Shelton, CT). The KBr sample disk was scanned with a scan number of 8 from 400 to 4000 cm^{-1} having a resolution of 2 cm^{-1}.

Powder X-ray diffraction (PXRD). Diffractograms of the powder samples were collected by the Bruker D8 Avance X-ray diffractometer (Germany). The source of PXRD was Cu Kα (1.542 Å) and the diffractometer was operated at 40 kV and 41 mA. The X-ray was passed through a 1-mm slit and the signal was passed through a 1-mm slit, a nickel filter, and another 0.1-mm slit. The detector type was a scintillation counter. The scanning rate was set at 0.05° 2θ/sec ranging from 5° to 35°. The quantity of sample used was around 20 to 30 mg.

Optical microscopy (OM). An optical microscope (SZII; Olympus, Tokyo, Japan) equipped with a CCD camera (SSC-DC50A; SONY, Tokyo, Japan) was used to take the images of the crystal habits.

Scanning electron microscopy (SEM). A scanning electron microscope (SEM) (Hitachi S-3500N, Tokyo, Japan) was used to observe the morphology of the crystals. Both secondary electron imaging (SEI) and backscattered electron imaging (BEI) were used for the SEM detector and the magnification was 15 to 300,000-fold. The operating pressure was 10^{-5} Pa vacuum and the voltage was 15.0 kV. All samples were mounted on a carbon conductive tape (Prod. No. 16073, TED Pella, Inc., Redding, CA) and then sputter-coated with gold (Hitachi E-1010 Ion Spotter, Tokyo, Japan) with a thickness of about 6 nm. The discharge current used was about 0 to 30 mA and the vacuum was around 10 Pa.

Electrical conductance. Electrical conductivity meter (CONSORT K611, Conductivity Instruments, Turnhout, Belgium) was used to monitor the conductivity of aspartic acid in a water–acetone system where acetone was added in the aqueous solution as an antisolvent. The electrical conductivity meter was calibrated with 0.01 M of KCl each time before use with an extrapolated conductivity of 1413 μS 1 M of KCl at 25°C. The purchased racemic aspartic acid was used to establish the calibration standards because it was inexpensive and the electrical conductivity values were independent from the chirality of aspartic acid. The linear relationship between electrical conductance and concentration: Conductivity (μS) = 2830.02 × Concentration (mol/L) + 3.32 with a correlation coefficient of 0.99, was established based on nine various concentrations of 5.8×10^{-4} M, 1.1×10^{-3} M, 2.3×10^{-3} M, 3.5×10^{-3} M, 4.6×10^{-3} M, 5.8×10^{-3} M, 6.9×10^{-3} M, 8.1×10^{-3} M, and 9.3×10^{-3} M of racemic aspartic acid in the solution of 60 mL of water + 140 mL of acetone at 25°C.

Experiments

Solubility values. About 10 mg of aspartic acid and alanine samples were weighed in a 20 mL scintillation vial. Drops of water were titrated carefully into the vial by a micropipette with intermittent shaking until all sample solids were just dissolved. The solubility value of samples in water at a given temperature was calculated as the weight of sample in a vial divided by the total volume of water added to a vial. The solubility values of aspartic acid and alanine samples in water were determined at 25° and 40°C. All temperatures were maintained and controlled by a water bath. Although the gravimetric method appeared to have an inherent inaccuracy of about ±10%, its advantages were its robustness, simplicity, without the need of performing any calibration, and without the concern of any hydrate formation and any racemic conglomerate-racemic compound transformation. All measurements were repeated at least three times.[2]

Crossovers. All crossover experiments were conducted at 40°C for 10 min. A standard 6-h, 40°C vacuum oven drying protocol was used to evaporate water and to generate solids from all aqueous solutions. The characteristic IR assignments[2] and the PXRD diffraction peaks[2] (i.e., 2θ = 11.8°, 25.5°, and 28.2° for racemic conglomerate aspartic acid, and 2θ = 13.2° and 19.5° for racemic compound aspartic acid) were used to distinguish racemic conglomerates from racemic compounds. However, from the previous literature,[13–15] IR spectra have shown discriminative peaks for the functional groups, such as -COO^- (in-plane bending), -COOH (in-plane bending), -CH_2 (rocking), -CN (stretching), -CH_2 (twisting) for aspartic acid, and -NH_2 (scissoring), -NH_2 (puckering) for alanine. Instead of employing PXRD, IR characterization was mainly used to identify racemic conglomerate and/or racemic compound, and conveniently determine the stability for racemic conglomerate.[2]

Since the solubility values of *dl*-aspartic acid, *d*- or *l*-aspartic acid, *dl*-alanine and *d*- or *l*-alanine in water at 40°C were about 10.1, 6.7, 200.7, and 169.9 mg/mL, respectively,[2,16] the clear solutions obtained after the 10-min incubation right before drying were unsaturated and should not contain any undissolved seeds.

Experimental procedures of Crossovers I between racemic conglomerate and racemic compound aspartic acid are described in Table 1, Crossovers II between racemic conglomerate and racemic compound alanine in Table 2, Crossovers III between *l*-aspartic acid and racemic compound aspartic acid in Table 3, Crossovers IV between *l*-alanine and racemic compound alanine in Table 4, and Crossovers V between $(l\text{-asp})_4$ and racemic compound aspartic acid in Table 5. Since $(l\text{-asp})_4$ was very expensive, it was used with a relatively small amount as templates or seeds only.

Although FTIR spectra and XRD patterns of *l*-aspartic acid and racemic conglomerate aspartic acid looked identical, we inferred that a mixture of *l*-aspartic acid and racemic conglomerate aspartic acid instead of pure *l*-aspartic acid or pure racemic conglomerate aspartic acid was obtained based on the component balance of *d*- and *l*-enantiomers.

Crystallization kinetics. Recrystallization of aspartic acid was carried out in a 250 cm^3 three-neck, round-bottom flask by antisolvent addition at 25°C. A known amount of aspartic acid was first dissolved in 60 mL of water. To further ensure a complete dissolution and to eliminate the invisible seeds, the unsaturated solution was warmed to 40°C for 30 min. It was then cooled back down to 25°C and stirred by a magnetic spin bar at 250 rpm for 1 h. Then 140 mL of acetone with or without seeds were added as an antisolvent. The total volume of 140 mL of acetone + 60 mL of water gave 195 mL of water–acetone solution. The electrical conductance of the resultant solution was monitored as a function of time. All experiments were run for at least three times to test for reproducibility.

Racemic compound aspartic acid.. A known aqueous solution of racemic compound aspartic acid with four different concentrations of 4.0, 3.7, 3.3, and 3.1 mg/mL was prepared and stirred by a magnetic spin bar at 250 rpm for 1 min. Because the solubility of racemic compound aspartic acid in the water–acetone solution was 0.30 mg/mL (i.e., $C^* = 2.2 \times 10^{-3}$ M) at 25°C, the initial concentrations, C_o, would become

TABLE 1. Crossovers I between racemic conglomerate and racemic compound aspartic acid

Experiments	Crystals yielded
(a) 3.0 mL of water containing 10.0 mg of racemic compound aspartic acid were added to 10.0 mg of racemic conglomerate aspartic acid	Racemic conglomerate (Fig. S1a)
(b) 3.0 mL of water containing 10.0 mg of racemic conglomerate aspartic acid were added to 10 mg racemic compound aspartic acid	Racemic compound (Fig. S1b)
(c) 3.0 mL of water were added to a solid mixture of 10.0 mg of racemic compound aspartic acid and 10.0 mg of racemic conglomerate aspartic acid	Racemic conglomerate (Fig. S1c)
(d) A 25°C nearly saturated aqueous solution by dissolving 5.0 mg of *d*-aspartic acid and 5.0 mg of *l*-aspartic acid in 1.3 mL of water was mixed with a nearly saturated aqueous solution prepared by dissolving 10.0 mg of *dl*-aspartic acid in 1.7 mL of water	A solid mixture of racemic conglomerate and racemic compound (Fig. S1d)
(e) 3 mL of water containing 10.0 mg of racemic conglomerate aspartic acid and 8.8 mg of succinic acid were added to 10 mg of racemic compound aspartic acid powders	A solid mixture of racemic conglomerate and racemic compound (Fig. S1e)

TABLE 2. Crossovers II between racemic conglomerate and racemic compound alanine

Experiments	Crystals yielded
(a) 3.0 mL of water containing 240.0 mg of racemic compound alanine were added to 240.0 mg of racemic conglomerate alanine crystals	Racemic compound (Fig. S2a)
(b) 3.0 mL of water containing 240.0 mg of racemic conglomerate alanine were added to 240.0 mg racemic compound alanine crystals	Racemic compound (Fig. S2b)
(c) 3.0 mL of water were added to a mixture of 240.0 mg of racemic compound alanine and 240.0 mg of racemic conglomerate alanine	Racemic compound (Fig. S2c)
(d) A 25°C nearly saturated aqueous solution by dissolving 120.0 mg of *d*-alanine and 120.0 mg of *l*-alanine in 1.3 mL of water was mixed with a nearly saturated aqueous solution prepared by dissolving 240.0 mg of *dl*-alanine in 1.5 mL of water	Racemic compound (Fig. S2d)

TABLE 3. Crossovers III between *l*-aspartic acid and racemic compound aspartic acid

Experiments	Crystals yielded
(a) 3.0 mL of water containing 10.0 mg of racemic compound aspartic acid were added to 10.0 mg of *l*-aspartic acid	A solid mixture of *l*-aspartic acid and racemic conglomerate aspartic acid (Fig. S3a)
(b) 3.0 mL of water containing 10.0 mg of *l*-aspartic acid were added to 10.0 mg of racemic compound aspartic acid crystals	A solid mixture of *l*-aspartic acid and racemic conglomerate aspartic acid (Fig. S3b)
(c) 3.0 mL of water were added to a mixture of 10.0 mg of *l*-aspartic acid and 10.0 mg of racemic compound aspartic acid	A solid mixture of *l*-aspartic acid and racemic conglomerate aspartic acid (Fig. S3c)
(d) A 25 °C nearly saturated aqueous solution by dissolving 7.0 mg of *l*-aspartic acid in 1.8 mL of water was mixed with a nearly saturated aqueous solution prepared by dissolving 7.0 mg of *dl*-aspartic acid in 1.2 mL of water	A solid mixture of *l*-aspartic acid and racemic conglomerate aspartic acid (Fig. S3d)

TABLE 4. Crossovers IV between *l*-alanine and racemic compound alanine

Experiments	Crystals yielded
(a) 3.0 mL of water containing 240.0 mg of racemic compound alanine were added to 240.0 mg of *l*-alanine	A solid mixture of *l*-alanine and racemic compound (Fig. S4a)
(b) 3.0 mL of water containing 240.0 mg of *l*-alanine were added to 240.0 mg of racemic compound alanine solids	A solid mixture of *l*-alanine and racemic compound (Fig. S4b)
(c) 3.0 mL of water were added to a mixture of 240.0 mg of *l*-alanine and 240.0 mg of racemic compound alanine	A solid mixture of *l*-alanine and racemic compound (Fig. S4c)
(d) A 25°C nearly saturated aqueous solution by dissolving 240.0 mg of *l*-alanine in 1.5 mL of water was mixed with a nearly saturated aqueous solution prepared by dissolving 240.0 mg of *dl*-aspartic acid in 1.5 mL of water	A solid mixture of *l*-alanine and racemic compound (Fig. S4d)

TABLE 5. Crossovers V between (*l*-asp)$_4$ and racemic aspartic acid

Experiments	Crystals yielded
(a) 2.0 mg of (*l*-asp)$_4$ were dissolved in 1.0 mL of water containing 2.0 mg of racemic compound aspartic acid	Racemic compound (Fig. S5a)
(b) 2.0 mg of (*l*-asp)$_4$ were dissolved in 1.0 mL of water containing 2.0 mg of racemic conglomerate aspartic acid	Racemic conglomerate (Fig. S5b)
(c) 14 mL of acetone antisolvent containing 0.24 mg of suspended (*l*-asp)$_4$ seeds were added to 6.0 mL of an aqueous solution of racemic compound aspartic acid with a concentration of 4.0 mg/mL while being stirred by a magnetic spin bar at 250 rpm for 1 min.	Racemic compound (Fig. S5c)
(d) 14 mL of acetone antisolvent containing 2.40 mg of suspended (*l*-asp)$_4$ seeds were added to 6.0 mL of an aqueous solution of racemic compound aspartic acid with a concentration of 4.0 mg/mL while being stirred by a magnetic spin bar at 250 rpm for 1 min.	Racemic compound (Fig. S5d)

9.3×10^{-3} M, 8.5×10^{-3} M, 7.7×10^{-3} M, and 7.1×10^{-3} M, which gave the corresponding supersaturation ratios, S_0 (i.e., C_0/C^*), of 4.15, 3.81, 3.46, and 3.20, respectively, in 195 mL of water–acetone solution.

Racemic compound aspartic acid seeded with l-aspartic acid.. 1 %wt% of *l*-aspartic acid (i.e., 0.01 × 60 mL × initial concentration of racemic compound aspartic acid = 2.4, 2.2, 2.0, and 1.9 mg, respectively) was premixed with 140 mL of antisolvent acetone. The acetone suspension was introduced to a known 60 mL aqueous solution of racemic aspartic acid with four different concentrations of 4.0, 3.7, 3.3, and 3.1 mg/mL of racemic aspartic acid while being stirred by a magnetic spin bar at 250 rpm for 1 min. The corresponding supersaturation ratios, S_0 (i.e., C_0/C^*), were 4.15, 3.81, 3.46, and 3.20, respectively, in 195 mL of water–acetone solution.

Racemic conglomerate aspartic acid.. A known aqueous solution of racemic conglomerate aspartic acid with four different concentrations of 4.0, 3.7, 3.3, and 3.1 mg/mL was prepared and stirred by a magnetic spin bar at 250 rpm for 1 min. Prior to the addition of acetone, all aqueous solutions of racemic conglomerate aspartic acid were incubated for 10 min at 25°C. The solubility of conglomerate aspartic acid in the water–acetone solution was 0.31 mg/mL (i.e., $C^* = 2.3 \times 10^{-3}$ M) at 25°C, and the corresponding supersaturation ratios, S_0 (i.e., C_0/C^*) are 3.97, 3.64, 3.31, and 3.06, respectively, in 195 mL of water–acetone solution.

l-Aspartic acid.. 140 mL of antisolvent acetone was added to a 60 mL aqueous solution of 2.0, 1.8, 1.7, and 1.5 mg/mL of *l*-aspartic acid while being stirred by a magnetic spin bar at 250 rpm for 1 min. The solubility of *l*-aspartic acid in water–acetone solution was 0.16 mg/mL (i.e., $C^* = 1.2 \times 10^{-3}$ M) at 25°C, the initial concentrations, C_0, would become 4.6×10^{-3} M, 4.2×10^{-3} M, 3.9×10^{-3} M, and 3.6×10^{-3} M, which gave the corresponding supersaturation ratios, S_0 (i.e., C_0/C^*), of 3.96, 3.64, 3.3, and 3.05, respectively, in 195 mL of water–acetone solution.

Racemic aspartic acid seeded with 1 %wt% (l-asp)$_4$.. 1 %wt% of (*l*-asp)$_4$ (i.e., 0.01 × 60 mL × initial concentration of racemic aspartic acid = 2.4 mg) was premixed with 140 mL of acetone, which served as an antisolvent. The acetone suspension was introduced to 60 mL aqueous solution of racemic aspartic acid with a concentration of 4.0 mg/mL of racemic aspartic acid while being stirred by a magnetic spin bar at 250 rpm for 1 min. The corresponding supersaturation ratios, S_0 (i.e., C_0/C^*), of 4.15 in 195 mL of water–acetone solution.

Morphological studies.. Although a statistically representative powder sample size of about 20 to 30 mg was used for PXRD to identify the racemate types, morphological studies of crystals were also employed for comparisons. 14 mL of acetone was added to 6 mL aqueous aspartic acid solution with a concentration of 4.0 mg/mL containing various molar or mass ratios of a racemic compound to a racemic conglomerate or a racemic compound to *l*-aspartic acid of 100:0, 80:20, 60:40, 40:60, 20:80, and 0:100 OM and SEM images of grown crystals were taken for further comparisons.

RESULTS AND DISCUSSION

Crossovers I Between Racemic Conglomerate and Racemic Compound Aspartic Acid

When all the solids were dissolved prior to mixing in the absence of seeds as in Crossovers I-d, a familiar situation[2] came about where a mixture of racemic conglomerate and racemic compound crystals was produced. This result suggested some sort of molecular association or "memory" existing in the starting solutions which could not be erased by instant mixing or diffusion. But when the temporarily suspended *d*- and *l*-enantiomorphs were present upon the instant addition of water as in Crossovers I-a, or when the temporarily suspended *d*- and *l*-enantiomorphs were separated out from the racemic compound solids upon the instant addition of water as in Crossovers I-c, it could facilitate the faster formation of less stable conglomerate kinetically due to the physicochemical properties of aspartic acid in water. This happened when RCS was in contact with the temporarily suspended *d*- and *l*-enantiomorphs through the surface templating effect. Therefore, a differentiation between the types of liquid solution generated from their corresponding solid phases does exist. This indicates that the history of preparing the solutions became very important for aspartic acid.

However, the surface templating effect here was different from the usual mechanism of seeding or epitaxy matching because no organized solid structures were deposited, but only liquid structures similar to a diffuse layer were loosely docked on the *d*- and *l*-enantiomorphs which, at the same time, were gradually dissolved away. The newly formed CS from the dissolution of conglomerate crystals and from the transformation of RCS by the templating effect would stabilize for 36 h at 25°C as evidenced by IR in our previous study,[2] which was one very important feature of aspartic acid. The transformation from CS to RCS of aspartic acid and solid state transition of racemic conglomerate to racemic compound aspartic acid will occur when the templating effect is completely eliminated, and then the clear solution will form thermodynamically stable racemic compound crystals. The relatively long-lived CS could not be erased by diffusion over the time course of vacuum evaporation at 40°C. Consequently, racemic conglomerate aspartic acid was crystallized out after water removal. As no surprise, the dissolution of racemic compound aspartic acid and their corresponding templating effect on the preexisting CS could also generate the thermodynamically favored RCS, which resulted in racemic aspartic acid upon drying. By comparing Crossovers I-b with Crossovers I-e, we could see that the presence of

succinic acid did help stabilize[2] the CS against the templating effect brought about by the solids of racemic compound aspartic acid, but not so much as to prevent their dissolution at all. Interestingly, the outcomes of Crossovers I-d and I-e could also be transformed into a racemic conglomerate by simply adding water to their solid products as indicated in Crossovers I-c. Therefore, only 1 out of 5 situations could definitely give racemic compound aspartic acid solids.

Crossovers II Between Racemic Conglomerate and Racemic Compound Alanine

To verify if the above experimental observations were indeed the distinctive features of aspartic acid, we also performed similar crossovers between racemic conglomerate and racemic compound alanine.

All alanine-related experiments gave racemic solids because alanine did not form a CS. Even if the templating effect and the dissolution of racemic conglomerate alanine did take place and gave the short-lived, liquid-like CS in the diffuse double layer, the liquid structure would become very unstable and instantly be randomized by diffusion. Therefore, all alanine nuclei must have grown directly from the same homogeneous racemic solution without any metastable liquid-like structure in transition as predicted by the classical nucleation theory (CNT).[17]

Since crossovers involving a racemic conglomerate and a racemic compound had equal amounts of *d*- and *l*-enantiomers in the solution, it would be intriguing to look at more realistic situations where there was an abundance of *l*-enantiomers (i.e., an insufficiency of *d*-enantiomers) in the supply. These situations would simulate the impact on the propagation of biochirality brought about by the enantioenrichment of *l*-enantiomers.

Crossovers III Between L-Aspartic Acid and Racemic Compound Aspartic Acid

In Crossovers III-a, *l*-aspartic acid solids also acted as templates to induce the formation of the LS when they came into contact with the RCS which was resolved into a LS and a *d*-aspartic acid solution (DS). Later removal of water by drying, racemic conglomerate solids with an excess amount of *l*-aspartic acid were obtained. In Crossovers III-b, the templating effect played no role in switching solution phase from the preformed LS to a RCS because of an insufficient supply in *d*-aspartic acid. A timepoint was finally reached where the LS and the RCS coexisted in the absence of solids. But later on, evaporation took place upon oven drying. *l*-Aspartic acid would crystallize out first from the LS due to its lower solubility value in water.[2] The *l*-aspartic acid solids would become the template to transform the RCS to the LS. As the LS was being formed, *d*-aspartic acid originally present in the RCS would be resolved and started to form the DS. Solids obtained from this kind of mixture of a large amount of LS and a small amount of DS resulted in *l*-aspartic acids and conglomerate aspartic acids. As water was added in Crossovers III-c, both the LS and RCS were being formed from the instant dissolution of *l*-aspartic acid and racemic compound aspartic acid, respectively. Although the racemic solids with a higher solubility of 10.1 mg/mL at 40°C in water and an insufficient supply in *d*-aspartic acid in total could not do much on the LS through the templating effect, the slower dissolution of *l*-aspartic acid solids with a lower solubility of 6.7 mg/mL at 40°C in water could do the otherwise on the RCS and definitely more so during the course of water removal upon drying by the same reasons given to Crossovers III-b. As for Crossovers III-d, only the templating effect of *l*-aspartic acid solids on both the LS and the RCS would be possible during the course of evaporation upon drying for the same reasons given to Crossovers III-b. Therefore, 0 out of 4 situations gave racemic aspartic acid solids.

To verify that the above observations were unique to aspartic acid systems, control experiments were performed on the alanine systems which were incapable of forming any molecular association in an aqueous solution.[2]

Crossovers IV Between L-Alanine and Racemic Compound Alanine

Since the solubility values of *dl*-alanine[16] and *d*- or *l*-alanine in water at 40°C were about 200.7 mg/mL and 169.9 mg/mL, respectively, the clear solutions obtained after the 10-min incubation right before drying were unsaturated and should not contain any undissolved seeds.

All experiments gave the same result of a solid mixture of *l*-alanine and racemic alanine because the liquid structures of LS + DS did not exist for alanine. Even if the templating effect and the dissolution of *l*-alanine and racemic alanine solids did take place and give the short-lived LS + DS in the diffuse double layer, the liquid structure would become very unstable and instantly randomized by diffusion to become LS + RCS because the number of *l*-alanine molecules was larger than the one of *d*-alanine molecules. Therefore, all alanine nuclei must have grown directly from the same stable homogeneous solution of LS + RCS (i.e., not pure RCS because of an insufficient supply of *d*-alanine) instead of growing from the unstable heterogeneous solution of LS + DS.

We have already shown that the enantioenrichment of *l*-aspartic acid by crystallization could lead to the propagation of biochirality (i.e., the generation of *l*-aspartic acid and/or racemic conglomerate aspartic acid from racemic compound aspartic acid) because of the templating effect brought about by the solids of enantiomorphs and the liquid structures created by the dissolution of enantiomorphs. But whether the enrichment of *l*-aspartic acid by polymerization could achieve the same results, tetrapeptides of aspartic acid $(l\text{-asp})_4$ would need to be used for the crossovers.

Crossovers V Between $(L\text{-Asp})_4$ and Racemic Aspartic Acid

The experimental results indicated that the RCS gave racemic solids and the CS racemic conglomerate crystals. The presence of $(l\text{-asp})_4$ played no role in disturbing the liquid structure or determining the final form. In comparison with other solid forms of aspartic acid monomers, $(l\text{-asp})_4$ did not act efficiently as templates or seeds. Perhaps short oligopeptides might only operate as templates for regioselective growth in the ensuing steps of chain elongation,[18] but not as nuclei for enantioseparation through crystallization in the racemic prebiotic world.

Crystallization Kinetics

The antisolvent crystallization pathways were all summarized in the tertiary phase diagrams (Fig. 1).

The preexistence of a liquid structure before nucleation would create a problem for the CNT[17] stemming from the

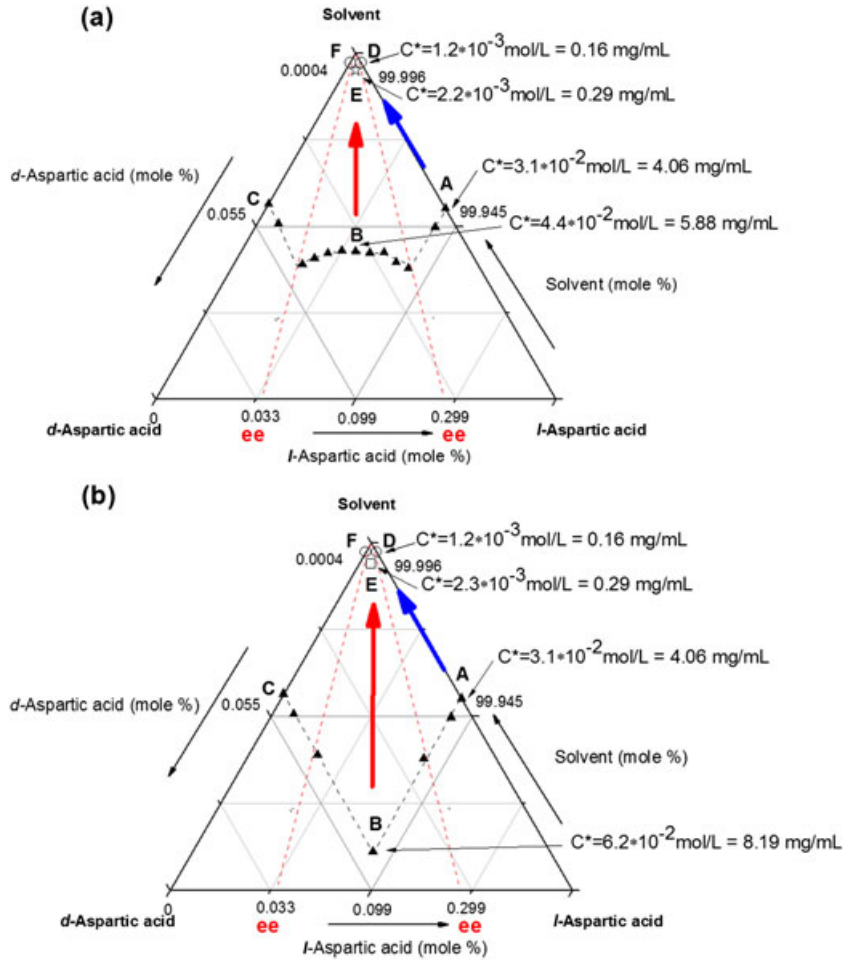

Fig. 1. Ternary phase diagrams for (**a**) the antisolvent crystallization pathway of traveling from a racemic compound aspartic acid forming system with or without seeds as denoted by Curve ABC in water to a racemic compound aspartic acid forming system as depicted by Points DEF in the water–acetone solution after the addition of acetone antisolvent as indicated by the red arrow. A solubility curve at 25°C in water is represented by a locus of ▲ denoted as Curve ABC. Points A and C are the solubility values of *l*- and *d*-aspartic acid ($C^* = 3.1 \times 10^{-2}$ mol/L = 4.06 mg/mL), respectively, and Point B is the solubility value of racemic compound aspartic acid ($C^* = 4.4 \times 10^{-2}$ mol/L = 5.88 mg/mL). A solubility curve at 25°C in 195 mL of a water–acetone solution is represented by a locus of ○, ☆ and ○, denoted as Curve DEF. Points D and F are the solubility values of *l*- and *d*-aspartic acid ($C^* = 1.2 \times 10^{-3}$ mol/L = 0.16 mg/mL) and Point E as denoted by ☆ is the solubility value of racemic aspartic acid ($C^* = 2.2 \times 10^{-3}$ mol/L = 0.29 mg/mL) in water–acetone solution (ee: two dashed lines going from the apex to the base of the triangle are the eutectic lines). (**b**) The antisolvent crystallization pathway of traveling from a racemic conglomerate aspartic acid forming system as denoted by Curve ABC in water to a racemic conglomerate aspartic acid forming system as depicted by Points DEF in water–acetone solution after the addition of acetone antisolvent as indicated by the red arrow. A solubility curve at 25°C in water is represented by a locus of ▲ denoted as Curve ABC. Points A and C are the solubility values of *l*- and *d*-aspartic acid ($C^* = 3.1 \times 10^{-2}$ mol/L = 4.06 mg/mL), respectively, and Point B is the solubility value of racemic conglomerate aspartic acid ($C^* = 6.2 \times 10^{-2}$ mol/L = 8.19 mg/mL). A solubility curve at 25°C in water–acetone solution is represented by a locus of ○, □, and ○ denoted as Curve DEF. Points D and F are the solubility values of *l*- and *d*-aspartic acid ($C^* = 1.2 \times 10^{-3}$ mol/L = 0.16 mg/mL) and Point E as denoted by □ is the solubility value of racemic conglomerate aspartic acid ($C^* = 2.3 \times 10^{-3}$ mol/L = 0.29 mg/mL) in water–acetone solution (ee: two dashed lines going from the apex to the base of the triangle are the eutectic lines). The identical antisolvent crystallization pathway of *l*-aspartic system was designated by a blue arrow in both (a) and (b).

belief in homogeneous nucleation,[19] as we will see shortly. The classical nucleation relationship stated that:

$$J = J_0 \exp\left[\frac{-16\pi\gamma^3 \upsilon^2}{3k^3T^3(\ln S_0)^2}\right] \quad (1)$$

where J is the rate of primary nucleation, J_0 is the preexponential factor (i.e., the number of molecules of the crystallizing phase in a unit volume × the frequency of molecular transport at the nucleus-liquid interface),[20] γ is the solution-solid interfacial energy, υ is the molecular volume (i.e., molecular weight/(density × Avogadro's number)), k is the Boltzmann's constant, T is the temperature, and S_0 is the initial supersaturation ratio (i.e., C_0/C^* = the initial bulk concentration of solutes/equilibrium solubility of solutes) may therefore be written:

$$\ln\tau = \ln t_n = -\ln J_0 + \left[\frac{16\pi\gamma^3\upsilon^2}{3k^3T^3}\right](\ln S_0)^{-2} \quad (2)$$

where τ is the induction period, and t_n is the nucleation time, which suggests that for a given temperature, a plot of ln τ versus $(\ln S_0)^{-2}$ should yield a straight line, the slope and the y-intercept of which should allow a value of the interfacial tension, γ, and a value of the preexponential factor to be calculated. The densities of racemic compound aspartic acid, racemic conglomerate aspartic acid, and *l*-aspartic acid are 1.645, 1.63991, and 1.63991 g/cm^3, respectively.[2]

The electrical conductance of water–acetone solution containing aspartic acid was linearly proportional to the concentration of the dissolved aspartic acid in the solution (Fig. 2). In general, experimental curves of concentration versus time exhibited a typical Z shape with three consecutive stages of the induction period, desupersaturation, and the

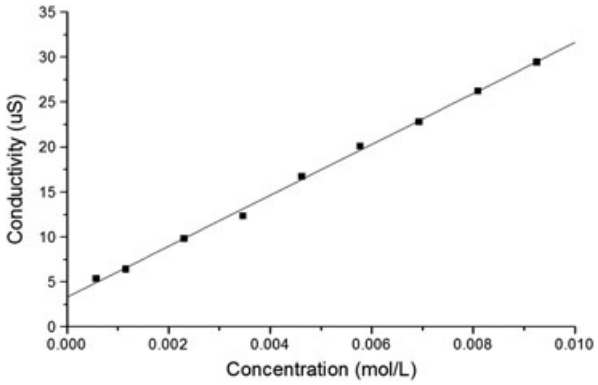

Fig. 2. Calibration of the electrical conductance vs. the concentration of the racemic compound aspartic acid in water–acetone solution at 25°C with a linear fit of $y = 2830.02x + 3.32$ with the value of a correlation coefficient of 0.99 was established.

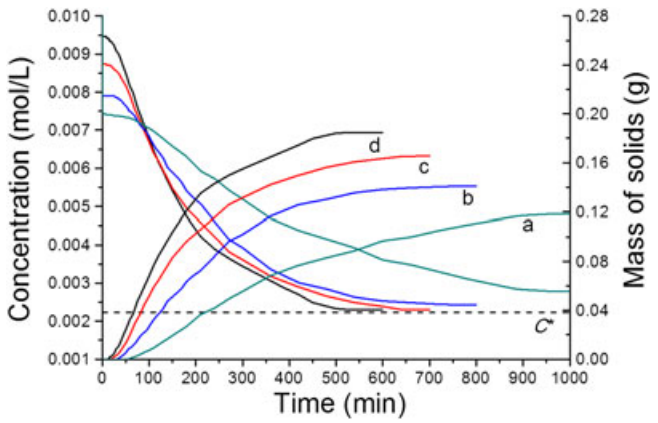

Fig. 3. Experimental Z-shaped curves of the concentration of an acetone–water racemic compound solution of pure aspartic acid vs. time and the calculated S-shaped curves of the crystal mass growth vs. time at $T = 25°C$ with initial supersaturation ratios of (a) $S_0 = 3.20$, (b) $S_0 = 3.46$, (c) $S_0 = 3.81$, and (d) $S_0 = 4.15$.

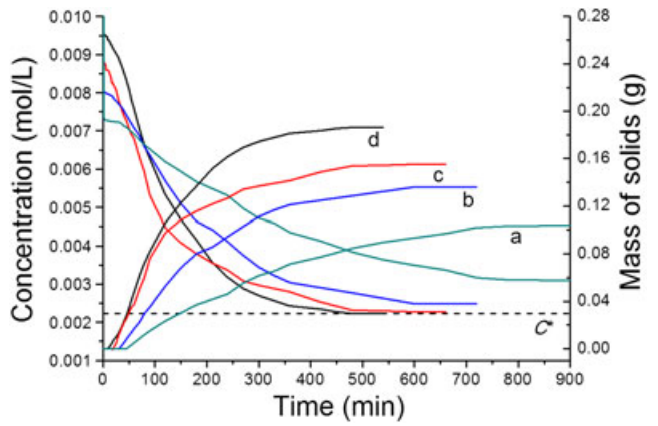

Fig. 4. Experimental Z-shaped curves of the concentration of an acetone–water racemic compound solution of aspartic acid vs. time and the calculated S-shaped curves of the crystal growth vs. time seeded with 1 %wt% of *l*-aspartic acid at $T = 25°C$ having initial supersaturation ratios of (a) $S_0 = 3.20$, (b) $S_0 = 3.46$, (c) $S_0 = 3.81$, and (d) $S_0 = 4.15$.

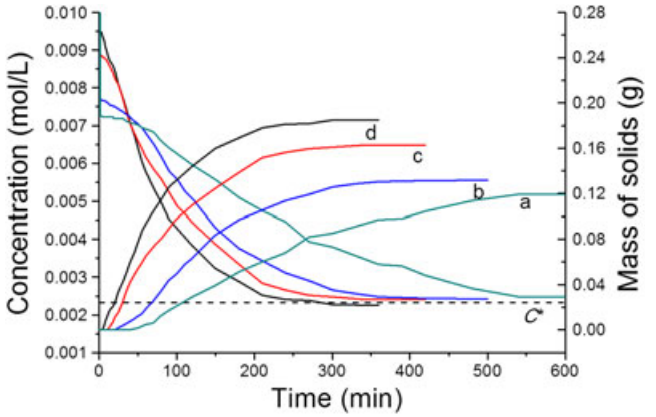

Fig. 5. Experimental Z-shaped curves of the concentration of an acetone–water racemic conglomerate solution of aspartic acid vs. time at $T = 25°C$ with initial supersaturation ratios of **(a)** $S_0 = 3.06$, **(b)** $S_0 = 3.31$, **(c)** $S_0 = 3.64$, and **(d)** $S_0 = 3.97$.

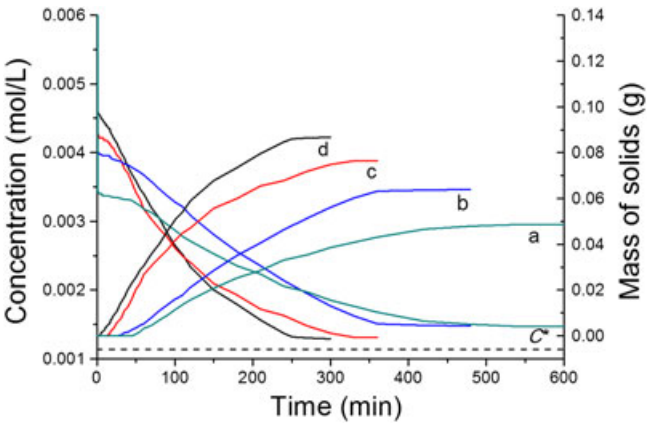

Fig. 6. Experimental Z-shaped curves of the concentration of an acetone–water *l*-aspartic solution of aspartic acid vs. time at $T = 25°C$ with initial supersaturation ratios of **(a)** $S_0 = 3.05$, **(b)** $S_0 = 3.30$, **(c)** $S_0 = 3.64$, and **(d)** $S_0 = 3.96$.

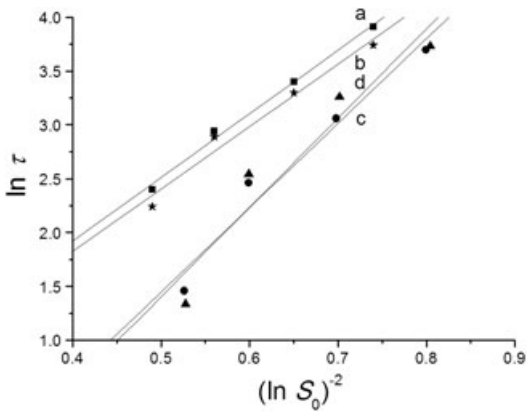

Fig. 7. $\ln \tau$ vs. $(\ln S_0)^{-2}$ plot of **(a)** pure racemic compound aspartic acid, **(b)** racemic compound aspartic acid with the addition of 1 %wt% *l*-aspartic acid seeds, **(c)** racemic conglomerate aspartic acid, and **(d)** pure *l*-aspartic acid, in an acetone–water solution at $T = 25°C$.

endpoint at a final equilibrium value of solubility, C^*, at 25°C (Figs. 3–6). The four sets of experiments were as follows: (i) racemic compound aspartic acid, (ii) racemic compound aspartic acid seeded with 1 %wt% of *l*-aspartic acid, (iii) racemic conglomerate aspartic acid, and (iv) *l*-aspartic acid, which has been described in the experimental section. The

TABLE 6. Tabulated values of S_0, τ, γ, and J_0 of (a) racemic aspartic acid, (b) racemic aspartic acid seeded with 1 wt % of *l*-aspartic acid, (c) racemic conglomerate aspartic acid, and (d) *l*-aspartic acid at $T = 25°C$, having different initial supersaturation ratios of S_0 in 195 mL of water-acetone solution

$S_0 = C/C^*$	τ (min)	γ ($\times 10^{-5}$ J/m^2)	J_0 (nucleus s^{-1} m^{-3})
Recrystallization of racemic aspartic acid			
3.20	54.67 ± 3.7	1101.83 ± 9.4	1.39 ± 0.2
3.46	32.33 ± 1.7		
3.81	20.33 ± 1.9		
4.15	12.67 ± 1.3		
Recrystallization of racemic aspartic acid seeded with 1 wt % *l*-aspartic acid			
3.20	44.33 ± 3.3	1126.99 ± 21.6	2.25 ± 0.5
3.46	28.33 ± 1.9		
3.81	17.06 ± 2.1		
4.15	9.26 ± 1.4		
Recrystallization of racemic conglomerate aspartic acid			
3.06	40.33 ± 3.6	1213.16 ± 25.2	12.31 ± 3.5
3.31	21.33 ± 2.6		
3.64	11.66 ± 1.2		
3.97	4.33 ± 0.8		
Recrystallization of *l*-aspartic acid			
3.05	41.67 ± 2.7	1204.26 ± 18.9	13.81 ± 1.5
3.30	26.00 ± 2.2		
3.64	12.67 ± 1.5		
3.96	3.83 ± 0.3		

TABLE 7. Tabulated values of S_0, ΔG_v, ΔG_{cr}, J, r_c, and i^* of (a) racemic aspartic acid, (b) racemic aspartic acid seeded with 1 wt % *l*-aspartic acid, (c) racemic conglomerate aspartic acid, and (d) *l*-aspartic acid at $T = 25°C$, having different initial supersaturation ratios of S_0 in 195 mL of water-acetone solution

$S_0 = C_0/C^*$	ΔG_v ($\times 10^5$ J/m^3)	ΔG_{cr} ($\times 10^{-22}$ J)	J ($\times 10^{-4}$ nucleus s^{-1} m^{-3})	r_c ($\times 10^{-10}$ m)	i^*
Recrystallization of racemic aspartic acid					
3.20	−358.40	178.07 ± 4.6	21.86 ± 2.4	6.19 ± 0.1	7.36 ± 0.3
3.46	−382.47	156.37 ± 3.9	37.02 ± 3.7	5.80 ± 0.1	6.05 ± 0.2
3.81	−412.16	134.65 ± 3.4	62.67 ± 5.3	5.38 ± 0.1	4.84 ± 0.2
4.15	−438.50	118.96 ± 3.0	91.70 ± 6.9	5.06 ± 0.1	4.02 ± 0.1
Recrystallization of racemic aspartic acid seeded with 1wt % *l*-aspartic acid					
3.20	−346.55	190.73 ± 11.0	16.96 ± 4.4	6.43 ± 0.2	8.27 ± 0.7
3.46	−369.83	167.48 ± 9.7	29.62 ± 6.8	6.02 ± 0.2	6.80 ± 0.6
3.81	−398.54	144.22 ± 8.3	51.78 ± 10.3	5.59 ± 0.2	5.38 ± 0.5
4.15	−424.00	127.41 ± 7.4	77.57 ± 13.7	5.25 ± 0.2	5.06 ± 0.4
Recrystallization of racemic conglomerate aspartic acid					
3.06	−337.28	257.36 ± 16.1	16.23 ± 6.1	7.20 ± 0.2	11.51 ± 1.1
3.31	−360.96	224.70 ± 14.1	35.30 ± 11.5	6.73 ± 0.2	9.47 ± 0.9
3.64	−389.62	196.86 ± 12.1	75.46 ± 21.3	6.24 ± 0.2	7.57 ± 0.7
3.97	−415.79	169.35 ± 10.6	132.42 ± 33.0	5.86 ± 0.2	6.28 ± 0.6
Recrystallization of *l*-aspartic acid					
3.05	−328.29	268.95 ± 5.5	19.993 ± 2.7	7.23 ± 0.1	11.74 ± 0.4
3.30	−351.82	234.32 ± 4.8	46.28 ± 5.3	6.74 ± 0.1	9.55 ± 0.3
3.64	−380.94	199.66 ± 4.1	107.32 ± 10.6	6.23 ± 0.1	7.51 ± 0.2
3.96	−408.37	174.73 ± 3.7	196.62 ± 18.1	5.83 ± 0.1	6.15 ± 0.2

electrical conductance of all curves was firstly converted into the concentration values through the calibration curve in Figure 2. They were then transformed into the concentration versus time curves as illustrated in Figures 3–6, respectively. In each set of experiments, the four different induction times were plotted against the four corresponding initial supersaturation ratios in a fashion of $\ln \tau$ vs. $(\ln S_0)^{-2}$ in Figure 7. γ and J_0 could then be estimated directly from the slope and y-intercept, respectively, from Figure 6, according to eq. (2) (Table 6). The free energy change for the phase transformation, ΔG_v, the energy required to form a critical size of cluster in nucleation, ΔG_{cr}, the rate of primary nucleation, J, the critical size, r_c, and the critical nucleus, i^*, could then be derived from γ and J_0 (Table 7).[19]

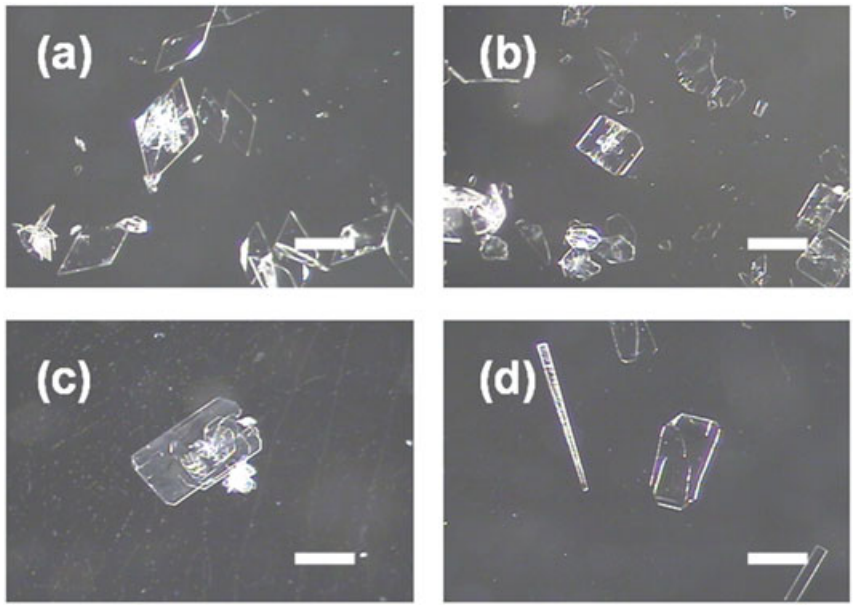

Fig. 8. Optical micrographs of crystals harvested towards the end of the recrystallization process in water–acetone solution of aspartic acid at 25°C: (**a**) racemic compound aspartic acid system at $S_O = 4.15$, (**b**) racemic compound aspartic acid seeded with 1 %wt% of *l*-aspartic acid at $S_O = 4.15$, (**c**) racemic conglomerate aspartic acid system at $S_O = 3.97$, and (**d**) *l*-aspartic acid at $S_O = 3.96$. (Scale bar = 200 μm).

Nucleation events were a consequence of thermodynamic, kinetic, and molecular recognition events. Usually, kinetic and molecular recognition events could be directly affected by the solubility and specific solvent properties such as polarizability, solubility parameter, or hydrogen bond propensity.[20,21] But sometimes, kinetic and molecular recognition events could also be influenced by the formation of micelles,[19] and the formation of the CS and RCS as in our case. The classical nucleation equation predicted that under a constant supersaturation, S_O, the rate of nucleation should be more rapid in systems with higher solubilities, C^*, because increases in solubility resulted in an increase in the preexponential factor, J_O or $N_O v$, and the probability of intermolecular collisions.[20] When a change in the solute from racemic conglomerate to racemic compound aspartic acid led to an increase in solubility (i.e., the solubility of conglomerate aspartic acid was actually 1/2 of the solubility of *d*- or *l*-aspartic acid, which was less than the one of racemic compound aspartic acid),[2] the interfacial energy, γ, decreased from $1213.16 \pm 25.2 \times 10^{-5}$ J/m^2 to $1101.83 \pm 9.4 \times 10^{-5}$ J/m^2 (Table 6) because of the affinity between crystallizing medium and crystal increased.

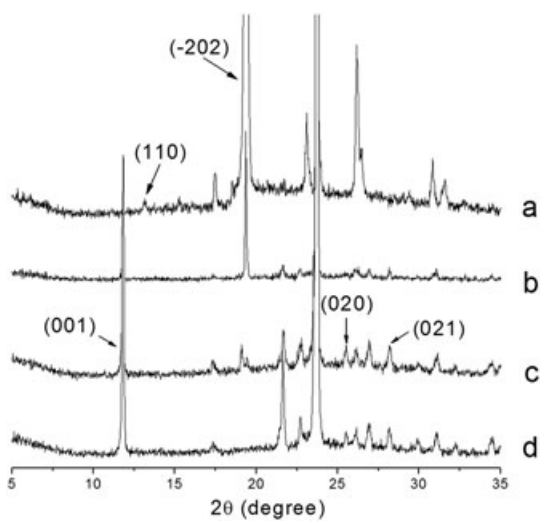

Fig. 9. PXRD diffractograms of crystals harvested towards the end of the recrystallization process in water–acetone solution of aspartic acid at 25°C: (**a**) racemic compound aspartic acid system at $S_O = 4.15$, (**b**) racemic compound aspartic acid seeded with 1 %wt% of *l*-aspartic acid at $S_O = 4.15$, (**c**) racemic conglomerate aspartic acid system at $S_O = 3.97$, and (**d**) *l*-aspartic acid at $S_O = 3.96$.

But an increase in the nucleation rate of aspartic acid with an increase in the solubility as predicted by eq. (1) was not experimentally observed. This was evidenced, for example, by $J = 91.70 \pm 6.9 \times 10^{-4}$ nucleus s^{-1} m^{-3} at $S_O = 4.15 \sim 4.0$ for the racemic compound aspartic acid and $J = 132.42 \pm 33.0 \times 10^{-4}$ nucleus s^{-1} m^{-3} at $S_O = 3.97 \sim 4.0$ for the racemic conglomerate aspartic acid in Table 7. The nucleation rate equation did not accurately predict aspartic acid nucleation behavior because it did not take the specific solute–solvent interactions for the racemic compound aspartic acid and for the racemic conglomerate aspartic acid which might control nucleation outcomes into account.

The racemic conglomerate aspartic acid and *l*-aspartic acid almost looked identical in τ, γ, and J_O at a given S_O (Table 6). Their J values differed greatly but still within the experimental errors because J was proportional to $\exp(-\gamma^3)$ as in eq. (1) at a given S_O (Table 7). Although a large discrepancy for S_O, τ, γ, J_O, ΔG_v, ΔG_{cr}, J, and r_c between racemic compound aspartic acid and the racemic compound aspartic seeded with 1 %wt% *l*-aspartic acid was not observed within the experimental errors (Tables 6 and 7), their outcomes were totally different. While racemic conglomerate aspartic acid gave platelets and the *l*-aspartic acid platelets and thin rods (Figs. 8c,d and 9c,d), racemic compound aspartic acid produced rhombus-shaped crystals and racemic compound aspartic acid seeded with 1 %wt% of *l*-aspartic acid generated square platelets of racemic conglomerate (Figs. 8a,b and 9a,b).

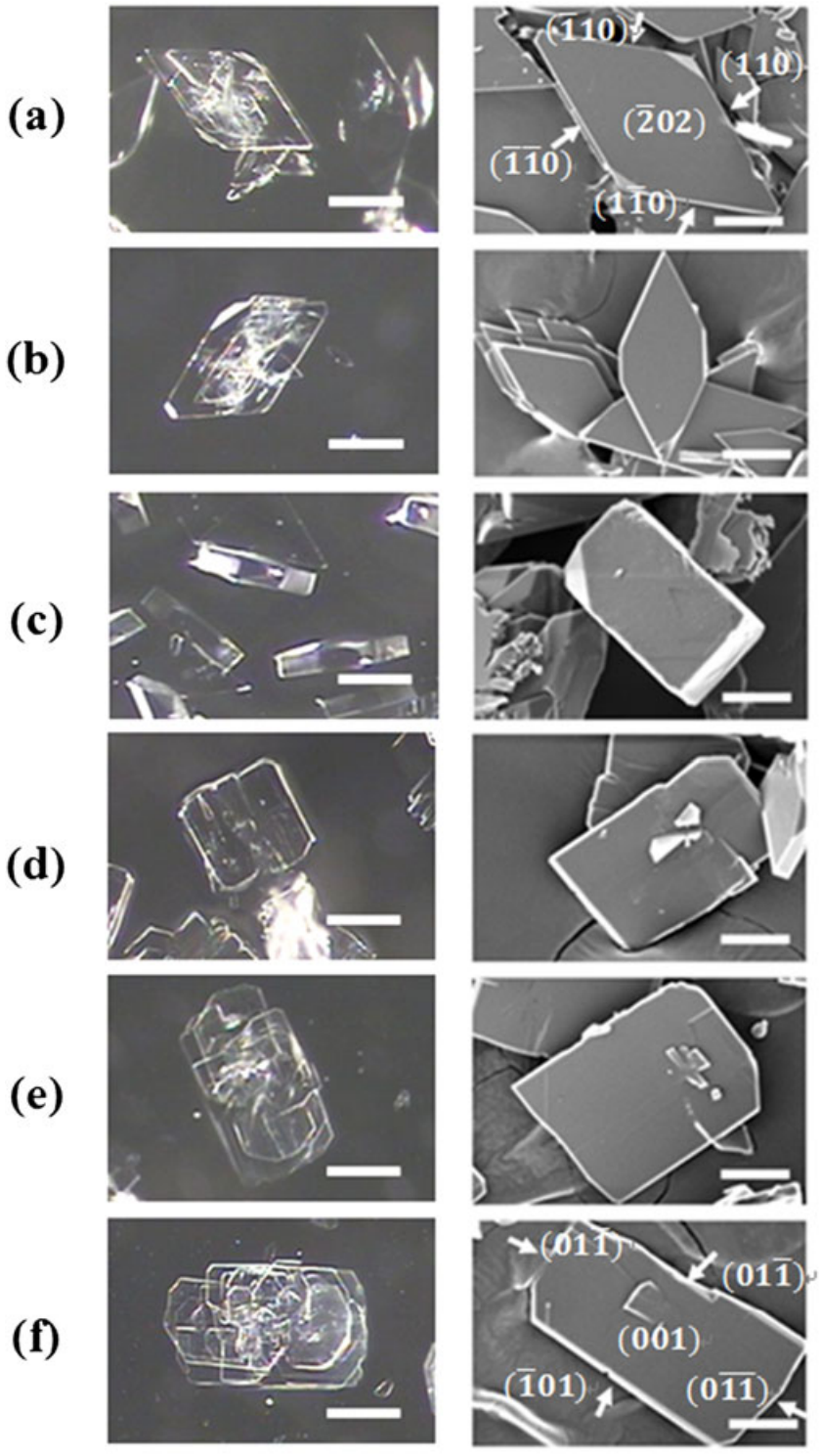

Fig. 10. Optical micrographs and SEM images of crystals grown from the water–acetone solutions containing aspartic acid of various racemic compound: racemic conglomerate ratios of (**a**) 100:0; (**b**) 80:20; (**c**) 60:40; (**d**) 40:60; (**e**) 20:80; and (**f**) 0:100 (OM scale bar = 200 μm and SEM scale bar = 100 μm).

By further comparing the OM images of the crystals harvest from the endpoints of the kinetics studies in Figure 8 with the morphology studies[22] in Figures 10 and 11, it was obvious that the racemic conglomerate did not transform to racemic compound aspartic acid over the course of the kinetics study. The crystal habit still remained as rectangular platelets (Fig. 10f). Or else, the crystal habits would have begun to transform to a square (Fig. 10d) and then to a rhombus shape (Fig. 10b) soon after the molar or mass ratio of racemic compound to racemic conglomerate in the solution deviated from 0:100. By the same token, the observed square platelets for the crystals grown from the kinetic study of

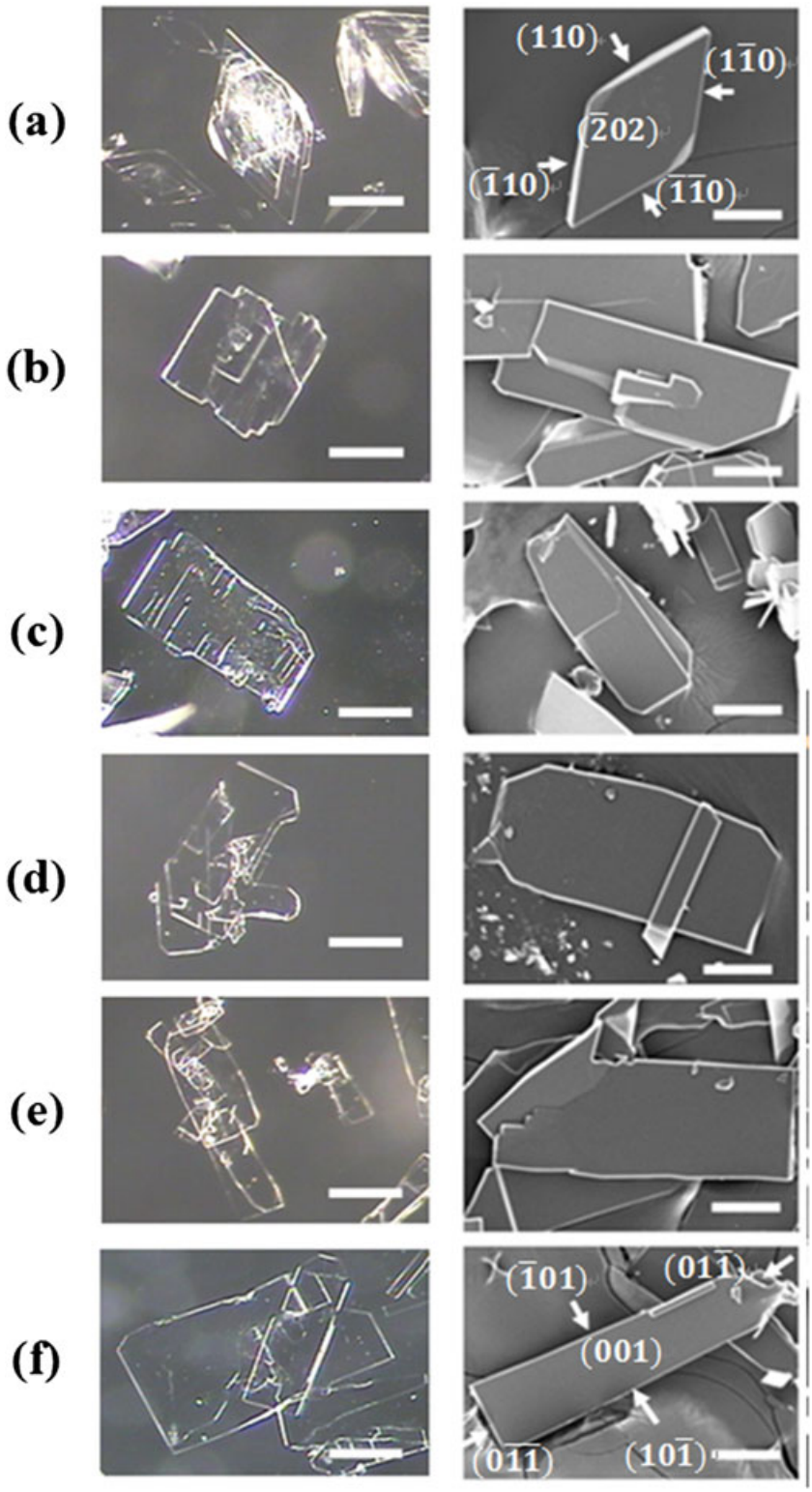

Fig. 11. Optical micrographs and SEM images of crystals grown from the water–acetone solutions containing aspartic acid of various racemic compound: *l*-aspartic acid ratios of **(a)** 100:0; **(b)** 80:20; **(c)** 60:40; **(d)** 40:60; **(e)** 20:80; and **(f)** 0:100 (OM scale bar = 200 μm and SEM scale bar = 100 μm).

racemic compound aspartic acid seeded with 1 %wt% *l*-aspartic acid (Fig. 8b) indicated that racemic compound aspartic acid must have transformed into racemic conglomerate (Fig. 10d–f), otherwise long rectangular platelets should have resulted (Fig. 11b–e).

According to the calculated eutectic ee of[23,24]:

$$ee^{eutectic} = \frac{1 - \left[\frac{\alpha^2}{4}\right]}{1 + \left[\frac{\alpha^2}{4}\right]} \text{x}100\% \quad (3)$$

where α = [*racemic compound*]/[*l-aspartic acid*] = (0.30 mg/mL) / (0.16 mg/mL) = 1.88, so $ee^{eutectic}$ = 6.5%. Under a normal

circumstance, for an enantioseparation of a racemic system by preferential crystallization to occur, the concentration of the enantiopure species must be above $ee^{eutectic}$. But in our case, the concentration of *l*-aspartic acid was 1 %wt%, which gave an *ee* value of 0.9% according to[24]:

$$ee = \frac{[L]-[D]}{[L]+[D]}\text{x}100\% = \frac{(120+2.4)mg - 120mg}{(120+2.4)mg + 120mg}\text{x}100\% \qquad (4)$$

which was way below 6.5%!

CONCLUSIONS

All of the experimental procedures discussed so far could be treated as a screening tool for probing the existence of any molecular association for other chiral molecules and solvent systems. The unusual property of the CS and the RCS of aspartic acid, and the templating effect of the aspartic acid crystals, made the transformation from racemic compound-to-racemic conglomerate highly probable with chances of at least 8 out of 9 (i.e., the number of types of experiments), but $(l\text{-asp})_4$ did not operate as a good template for inducing enantioseparation of racemic aspartic acid by crystallization. It was found that only 1 %wt% of *l*-aspartic acid solid seeds was adequate to switch racemic compound to a racemic conglomerate aspartic acid system. Seemingly, the decrease in aspartic acid nucleation rate with increasing solubility could only be explained by the nonclassical crystallization theory after taking the nonhomogeneity of the CS into account.

ACKNOWLEDGMENT

We are grateful for the research grant from the National Science Council of Taiwan, R. O. C. (NSC-101-2221-E-008-102). We thank Ms. Jui-Mei Huang for assistance with DSC and TGA, Ms. Shew-Jen Weng for PXRD, and Ms. Ching-Tien Lin for SEM. All with the Precision Instrument Center at National Central University are gratefully acknowledged. This article was inspired by my wife Daisy, my two sons Jeremiah and Kyle, and all the people at National Central University.

LITERATURE CITED

1. Jacques J, Collet A, Wilen SH. Binary mixtures of enantiomers. In: Enantiomers, racemates, and resolutions. New York: John Wiley & Sons; 1981. p 81.
2. Lee T, Lin Y-K. The origin of life and the crystallization of aspartic acid in water. Cryst Growth Des 2010;10:1652–1660.
3. He Q, Rohani S, Zhu J, Gomaa H. Crystallization of the racemic compound and conglomerate of (*RS*)-2-Chloromandelic acid. Cryst Growth Des 2010;10:5136–5145.
4. Van Eupen JThH, Elffrink WWJ, Keltjens R, Bennema P, de Gelder P, Smits JMM, van Eck ERH, Kentgens APM, Deij MA, Meekes H, Vlieg E. Polymorphism and migratory chiral resolution of the free base of venlafaxine. a remarkable topotactical solid state transition from a racemate to a racemic conglomerate. Cryst Growth Des 2008;8:71–79.
5. Mercier N, Barres A-L, Giffard M, Rau I, Kajzar F, Sahraoui B. Conglomerate-to-true-racemate reversible solid-state transition in crystals of an organic disulfide-based iodoplumbate. Angew Chem Int Ed 2006;45:2100–2103.
6. Viedma C. Enantiomeric crystallization from DL-aspartic and DL-glutamic acids: implications for biomolecular chirality in the origin of life. Origins Life Evol Biospheres 2001;31:501–509.
7. Klussmann M, Iwamura H, Mathew SP, Wells Jr DH, Pandya U, Armstrong A, Blackmond DG. Thermodynamic control of asymmetric amplification in amino acid catalysis. Nature 2006;441:621–623.
8. Viedma C, Ortiz JE, de Torres T, Izumi T, Blackmond DG. Evolution of solid phase homochirality for a proteinogenic amino acid. J Am Chem Soc 2008;130:15274–15275.
9. Koch KJ, Gozzo FC, Nanita SC, Takats Z, Eberlin MN, Graham Cooks R. Chiral transmission between amino acids: chirally selective amino acid substitution in the serine octamer as a possible step in homochirogenesis. Angew Chem Int Ed 2002;41:1721–1724.
10. Welch CJ. Formation of highly enantioenriched microenvironments by stochastic sorting of conglomerate crystals: a plausible mechanism for generation of enantioenrichment on the prebiotic earth. Chirality 2001;13:425–427.
11. Weissbuch I, Illos RA, Bolbach G, Lahav M. Racemic β-sheets as templates of relevance to the origin of homochirality of peptides: lessons from crystal chemistry. Acc Chem Res 2009;42:1128–1140.
12. Zbaida D, Lahav M, Drauz K, Knaup G, Kottenhahn M. A cyclic continuous process for converting conglomerates into optically pure enantiomers by crystallization and dissolution with the assistance of 'tailor made' polymers. Tetrahedron 2000;56:6645–6649.
13. Lōpez Navarrete JT, Hernández V, Ramírez FJ. IR and Raman spectra of L-aspartic acid and isotopic derivatives. Biopolymers 1994;34:1065–1077.
14. Jamieson MJ, Cooper SJ, Miller AF, Holt SA. Neutron reflectivity and external reflection FTIR studies of DL-aspartic acid crystallization beneath nylon 6 spread films. Langmuir 2004;20:3593–3600.
15. Kumar S, Rai AK, Rai SB, Rai DK, Singh AN, Singh VB. Infrared, Raman and electronic spectra of alanine: a comparison with ab intio calculation. J Mol Struct 2006;791:23–29.
16. Dunn MS, Ross FJ, Read LS. The solubility of the amino acids in water. J Biol Chem 1933;103:579–595.
17. Zhang TH, Liu XY. Nucleation: What happens at the initial stage? Angew Chem Int Ed 2009:48:1308–1312.
18. Weissbuch I, Illos RA, Bolbach G, Lahav M. Racemic β-sheets as templates of relevance to the origin of homochirality of peptides: lessons from crystal chemistry. Acc Chem Res 2009;42:1128–1140.
19. Lee T, Chen Y-H, Wang Y-W. Effects of homochiral molecules of (S)-(+)-ibuprofen and (S)-(−)-sodium ibuprofen dihydrate on the crystallization kinetics of racemic (R,S)-(±)-sodium ibuprofen dihydrate. Cryst Growth Des 2008;8:415–426.
20. Kelly RC, Rodríguez-Hornedo N. Solvent effects on the crystallization and preferential nucleation of carbamazepine anhydrous polymorphs: a molecular recognition perspective. Org Proc Res Dev 2009;13:1291–1300.
21. Musumeci D, Hunter CA, McCabe JF. Solvent effects on acridine polymorphism. Cryst Growth Des 2010;10:1661–1664.
22. Weissbuch I, Kuzmenko I, Vaida M, Zait S, Leiserowitz L, Lahav M. Twinned crystals of enantiomorphs morphology of racemic alanine induced by optically resolved α-amino acids; a stereochemical probe for the early stages of crystal nucleation. Chem Mater 1994;6:1258–1268.
23. Klussmann M, Izumi T, White AJP, Armstrong A, Blackmond D. Emergence of solution-phase homochirality via crystal engineering of amino acids. J Am Chem Soc 2007;129:7657–7660.
24. Wang Y, Chen A-M. Enantioenrichment by crystallization. Org Proc Res Dev 2008;12:282–290.